HHS Public Access

Author manuscript

Mol Psychiatry. Author manuscript; available in PMC 2014 July 01.

Published in final edited form as:

Mol Psychiatry. 2014 January ; 19(1): 99–107. doi:10.1038/mp.2013.112.

Neuroanatomical Phenotypes in a Mouse Model of the 22q11.2 Microdeletion

J. Ellegood[#1], **S. Markx**[#3], **J.P. Lerch**[1,2], **P.E. Steadman**[1,2], **C. Genç**[4], **F Provenzano**[5], **S.A. Kushner**[4], **R.M. Henkelman**[1,2], **M. Karayiorgou**[3], and **J.A. Gogos**[3]

[1]Mouse Imaging Centre, Hospital for Sick Children, Toronto, Ontario, Canada [2]Department of Medical Biophysics, University of Toronto, Toronto, Ontario Canada [3]Department of Psychiatry, College of Physicians and Surgeons, Columbia University, New York, New York, USA [4]Department of Psychiatry, Erasmus Medical Center, The Netherlands [5]Department of Department of Biomedical Engineering, College of Physicians and Surgeons, Columbia University, New York, New York, USA

[#] These authors contributed equally to this work.

Abstract

Recurrent deletions at the 22q11.2 locus have been established as a strong genetic risk factor for the development of schizophrenia and cognitive dysfunction. Individuals with 22q11.2 deletions have a range of well-defined volumetric abnormalities in a number of critical brain structures. A mouse model of the 22q11.2 deletion (*Df(16)A*$^{+/-}$) has previously been utilized to characterize disease-associated abnormalities on synaptic, cellular, neurocircuitry, and behavioral levels. We performed a high-resolution MRI analysis of mutant mice compared with wild-type (WT) littermates. Our analysis revealed a striking similarity in the specific volumetric changes of *Df(16)A*$^{+/-}$ mice compared with human 22q11.2 deletion carriers, including in cortico-cerebellar, cortico-striatal, and cortico-limbic circuits. In addition, higher resolution compared with neuroimaging in human subjects allowed detection of previously unknown subtle local differences. The cerebellar findings in *Df(16)A*$^{+/-}$ mice are particularly instructive as they are localized to specific areas within both the deep cerebellar nuclei and the cerebellar cortex. Our study indicates that the *Df(16)A*$^{+/-}$ mouse model recapitulates most of the hallmark neuroanatomical changes observed in 22q11.2 deletion carriers. Our findings will help guide the design and interpretation of additional complementary studies and thereby advance our understanding of the abnormal brain development underlying the emergence of 22q11.2 deletion-associated psychiatric and cognitive symptoms.

Introduction

The 22q11.2 deletion occur in approximately 1 in 2,000–4,000 live births[1]. The vast majority of them (~90%) are 3 megabases (Mb) in size and contain approximately 60 known

Corresponding authors: Maria Karayiorgou (mk2758@columbia.edu) or Joseph A. Gogos (jag90@columbia.edu) .

genes, while a smaller fraction (~8%) are 1.5Mb in size and contain approximately 28 known genes[1]. Most of the genes in the 22q11.2 locus are expressed in the brain throughout development (http://www.brain-map.org/).

The phenotype associated with 22q11.2 deletions is variable [1]. Phenotypic variability may be partially due to breakpoint heterogeneity or other genetic, environmental and stochastic factors. A strong link has been established between 22q11.2 deletion, cognitive dysfunction, and psychiatric disorders. Children with the deletion have specific behavioral impairments and exhibit a spectrum of deficits in cognitive abilities [1]. Adults with 22q11.2 deletions have a high risk of developing schizophrenia, approximately 25–31 times that of the general population. Indeed, 22q11.2 deletions are consistently found enriched in schizophrenia cohorts (ICS 2008) [2] accounting for 1–2% of non-familial (*i.e.*, sporadic) cases of schizophrenia [3, 4]. In contrast, no such enrichment has been reported in cohorts of patients with autism spectrum disorders [5] or bipolar disorder [6]. Furthermore, it has been suggested that the 1.5Mb deletion is the minimal region that contains most of the genes that can account for the increased risk of schizophrenia among 22q11.2 deletion carriers [1, 3].

A mouse model carrying a hemizygous 1.3-Mb chromosomal deficiency (*Df(16)A*$^{+/-}$) syntenic to the 1.5-Mb human 22q11.2 deletion and encompassing 27 genes has been previously generated and extensively investigated [7-12]. Behavioral characterization of the *Df(16)A*$^{+/-}$ mice has revealed specific deficits in sensorimotor gating, working memory, and fear conditioning [13]. Furthermore, several studies of the *Df(16)A*$^{+/-}$ mice have consistently shown modest differences in corticogenesis, relatively widespread deficits in dendritic complexity and spine density, as well as region-specific alterations in short- and long- term synaptic plasticity. *Df(16)A*$^{+/-}$ mice also demonstrate a diminished synchrony between the hippocampus and medial pre-frontal cortex activity during a task that relies on communication between these two structures, indicative of long-range functional connectivity impairments resulting from 22q11.2 deletions.

Due to the high evolutionary conservation between the human 22q11.2 locus and the syntenic region on mouse chromosome 16, which ensures that *Df(16)A* disrupts most of the crucial genes underlying the 22q11.2-associated phenotypes [13]. The *Df(16)A*$^{+/-}$ mouse model has strong *construct validity*. Whether this model also shows strong *face validity, i.e.*, recapitulation of some of the essential features of the disorder in humans, is more difficult to establish. Behavioral assays suggest that *Df(16)A*$^{+/-}$ mice and 22q11.2 deletion carriers share deficits in some broadly defined cognitive domains. However, compared to behavior, neuroanatomical features are generally more directly associated with the mutation and more highly analogous between mouse models and human subjects [14]. Indeed, various neuroanatomical phenotypes have been traditionally used to establish face validity in genetic mouse models of neurological disorders such as Huntington's disease, Alzheimer's disease and Parkinson's disease [15-17]. Similarly, replication of key neuroanatomical findings in genetic mouse models of neuropsychiatric and neurodevelopmental diseases is important for three reasons: First, it can provide confidence that a mouse model recapitulates the core pathophysiology of the disease and can therefore be useful in furthering our understanding of disease etiology. Second, it can provide reliable biomarkers that can facilitate translational studies including drug development efforts. Third, high-resolution magnetic

resonance imaging (MRI) is capable of detecting very subtle differences in brain structure and volume, allowing a more detailed examination of neuroanatomical features compared to human subjects [18, 19]. High-resolution neuroanatomical phenotyping has enabled detection of subtle volumetric brain changes in 17 mouse models in a sample of 19 different mouse behavioral mutants [20] and more recently in a number of genetic mouse models related to autism spectrum disorders, including Fragile X Syndrome [21], 16p11.2 deletion [22], and Neuroligin R541 knockin [23].

22q11.2 deletion carriers show a range of well-defined neuroanatomical abnormalities [2, 11, 24], for which non-invasive brain imaging studies have replicated specific volumetric and structural brain abnormalities. These include ventricular enlargement, a decrease in volume of both cerebral and cerebellar cortices, and an increase in striatal volume. Interestingly, some of these neuroanatomical findings have also been described in patients with schizophrenia although it remains unclear whether this neuroanatomical profile is related to the development of schizophrenia in 22q11.2 deletion carriers or whether it represents an independent manifestation of aberrant brain development. Regardless, in order to establish whether the *Df(16)A*$^{+/-}$ mouse model shows face validity, it is critical to evaluate whether the cardinal neuroanatomical features associated with the human 22q11.2 deletions –or at least a subset of them– are faithfully recapitulated in the mouse model.

Although no gross anatomical brain abnormalities have been described in *Df(16)A*$^{+/-}$ mice [3, 4, 7], brain structure at the mesoscopic level has never previously been examined systematically in these mice. Furthermore, it has also remained unknown whether the neuroanatomical changes found in human carriers of the 22q11.2 deletions are also present in the *Df(16)A*$^{+/-}$ mice. Therefore, we performed high-resolution MRI imaging of the *Df(16)A*$^{+/-}$ mouse model in an effort to define observable neuroanatomical features through a whole-brain unbiased analysis. Moreover, we carried out an extensive review of the MRI neuroimaging literature through which we demonstrate that the *Df(16)A*$^{+/-}$ mice harbor some of the most common neuroanatomical findings that have been described in human 22q11.2 deletion carriers. Our analysis confirms that the *Df(16)A*$^{+/-}$ mouse model has strong face validity by demonstrating that it clearly recapitulates several of the essential features of abnormal brain anatomy associated with human 22q11.2 deletions. Importantly, higher resolution compared with neuroimaging in human subjects allowed detection of previously unknown subtle local differences, including ones localized to specific areas within both the deep cerebellar nuclei and the cerebellar cortex

Methods

Mice

Mice have been described previously [5, 7, 8] and were bred at Columbia University (New York, NY). Mutant mice carry a hemizygous 1.3-Mb chromosomal deficiency (*Df(16)A*$^{+/-}$), which ranges from the *Dgcr2* gene to *Hira* and spans a segment syntenic to the 1.5-Mb human 22q11.2 deletion, encompassing 27 genes [6, 7]. The mutation has been backcrossed to C57BL/6 background for over 15 generations. Twenty male mice (10 *Df(16)A*$^{+/-}$ and 10 wildtype WT littermates) aged 14 to 24 weeks were perfused for MRI imaging.

Specimen Preparation

Mice were anesthetized with a mixture of ketamine and xylazine and then intracardially perfused with 30 mL of 0.1 M PBS containing 10 U/mL heparin (Sigma) and 2mM Prohance (a gadolinium contrast agent) (Bracco Diagnostics) [25, 26]. After perfusion, the mice were decapitated and the skin, lower jaw, ears, and cartilaginous nose tip were removed. The brain was left within the skull to eliminate any deformities that would be caused by its removal. The brain within the skull was incubated overnight at 4°C in 4% PFA containing 2mM of Prohance. Subsequently, the specimens were transferred to 0.1 M PBS containing 2 mM Prohance and 0.02% sodium azide for at least 7 days prior to MRI scanning. Perfusions were conducted at Columbia University in New York, after which the specimens were shipped overnight to the Mouse Imaging Centre (MICe) in Toronto where they were promptly stored at 4°C until scanning.

MRI Scanning

Images were acquired on a 7 Tesla MRI scanner (Varian Inc., Pao Alto, CA) with a 40 cm bore diameter. An in-house custom-built solenoid array was used to acquire all images. The solenoid array contains 16 individual transmit and receive coils, which allow the acquisition of images from 16 separate samples in one overnight session [26, 27]. Parameters used in the MRI scan were optimized for gray/white matter contrast and high efficiency. The sequence used was a T2 weighted 3D fast spin echo (FSE), with a TR of 200ms, an echo train length of 6, an effective TE of 42 ms, a field of view (FOV) of 25 mm × 28 mm × 14 mm, and a matrix size of 450 × 504 × 250, which leads to an isotropic resolution of 56 μm. In the first phase encode dimension, consecutive k-space lines were acquired with alternating echoes to move discontinuity related ghosting artifacts to the edges of the FOV [28]. This sequence requires oversampling of the phase encode dimension by a factor of two to avoid the interference of these artifacts. The FOV direction was subsequently cropped to 14 mm after reconstruction. Total imaging time for the acquisition was 11.7 hours [26].

Registration and Analysis

To test for any volumetric changes in *Df(16)A*$^{+/-}$ compared to WT mice images from the MRI scans were linearly (6 parameter followed by a 12 parameter) and subsequently non-linearly, registered. All scans were then re-sampled with the appropriate transform and averaged to create a population atlas, which represents the average anatomy of all brains. Registrations were performed with a combination of the mni_autoreg tools [29] and ANTS[30, 31]. The result of this registration is to have all scans deformed into exact alignment with each other in an unbiased fashion. This allows for the analysis of the deformations needed to take each individual brain into the final atlas space, the goal being to model how the deformation fields relate to genotype [32]. The Jacobian determinants of the deformation fields are then used to estimate the volume changes in each voxel. Significant regional volume changes can then be calculated in two different ways. First, regional measurements can be calculated by registering a pre-existing classified MRI atlas on to the population atlas, which allows for the volume measurement of 62 different brain regions. The 62 regions in the classified atlas include the cortical lobes, large white matter structures (*i.e.*, the corpus callosum), ventricles, cerebellum, brain stem structures, and olfactory bulbs [33].

The regions volumes were then assessed in all brains, as a percentage of total brain volume. Second, individual voxel measurements can be calculated from comparisons of the Jacobian determinants in a specific voxel between *Df(16)A*+/- and WT mice. All statistical analysis was performed in the R statistical environment (www.r-project.org). Multiple comparisons were controlled for by using either the False Discovery Rate (FDR) [34] for the regional comparisons, or [35] for the voxel-wise whole-brain Threshold Free Cluster Enhancement (TFCE) comparisons.

Results

The total brain volume was not significantly different between *Df(16)A*$^{+/-}$ and WT littermates mice (*Df(16)A*$^{+/-}$: 470 ± 16 mm^3, WT: 468 ± 14 mm^3). In order to account for individual brain sizes, relative volumes were compared between groups for the 62 different regions examined [33]. Thirteen of the 62 regions were found to be significantly different at an FDR threshold of 15% ($q < 0.15$) and 9 were found to be significantly different at 10% ($q < 0.10$) (Supplemental Table 1). Figure 1 shows the normalized percent difference for all 13 regions in comparison to WT littermates. The relative volumes of all 62 regions are shown in Supplementary Table 1, with their percent difference and corresponding q-values. Supplementary Table 2 shows the 62 regions, divided when possible, into left and right sides. The most prominent regional changes were seen in the cerebellar cortex, cortical spinal tract, cuneate nucleus, globus pallidus, lateral olfactory tract, pontine nucleus, posterior commissure, striatum, superior olivary complex, and third ventricle.

Many of these brain regions are also affected in humans with 22q11.2 deletions (see discussion). Table 1 lists volumetric changes found in *Df(16)A*$^{+/-}$ mice and compares them to the most common volumetric findings in 22q11.2 deletion carriers (with or without schizophrenia) and in subjects with schizophrenia who are known not to harbor a 22q11.2 deletion. Figure 2A,B illustrates brain areas where there is considerable overlap between the neuroimaging findings of 22q11.2 human carriers and the *Df(16)A*$^{+/-}$ mouse model. Prominent convergence is seen in the cerebellar cortex (Figure 2C), globus pallidus (Figure 2D), striatum (Figure 2E) and third ventricle (Figure 2F), all of which demonstrate similar volumetric changes in human 22q11.2 deletion carriers and *Df(16)A*$^{+/-}$ mice. Similarly convergent volumetric changes were also observed in the amygdala and the frontal lobe of the *Df(16)A*$^{+/-}$ mice (Figure 2). Overall, several of the core manifestations of the neuroanatomical alterations caused by 22q11.2 deletions in human subjects were also observed in the *Df(16)A*$^{+/-}$ mice. While certain brain structures were demonstrated to have a significant volumetric increase (*i.e.*, striatum, globus palldius, 3rd ventricle, and part of the frontal lobe), other regions were shown to have a significant decrease in volume (*i.e.*, cerebellum, amygdala, and part of the frontal lobe, including the frontal association cortex). The fact that multiple hallmark neuroanatomical findings in individuals with the 22q11.2 deletion are faithfully recapitulated confirms the face validity of the *Df(16)A*$^{+/-}$ mouse model.

In addition to volumetric measurements of the 62 different regions, we also performed a voxel-wise analysis to look at the differences within brain structures. The voxel-wise analysis revealed striking differences between the *Df(16)A*$^{+/-}$ mice and WT littermates

(Figure 3). Overall, the strongest differences were found in the cerebellum. The cerebellar cortex as a whole was 5% smaller in relative volume in the *Df(16)A*$^{+/-}$ mice, and within the cerebellum the voxel-wise analysis revealed several distinctly affected subregions. Affected bilateral hemispheric areas included the flocculous and para-flocculus, crus I dorsal surface, and medial aspects of the anterior lobule. Within the vermis, lobules IV/V, IX and X showed robust volume decreases in the *Df(16)A*$^{+/-}$ mice compared with WT mice. From these areas, the flocculus and para-flocculus were the most significantly affected areas within the cerebellum (Figure 4). The superior vestibular and vestibulocerebellar nuclei showed bilateral volumetric decrease as well (Figure 4C).

The amygdala did not display a significant overall volumetric difference between *Df(16)A*$^{+/-}$ and control mice. However, the voxel-wise measurements demonstrated a significant volumetric reduction of a region located in the anterior section of the amygdala (Figures 3C–E). Reductions of amygdala volume have been described both in pediatric populations with 22q11.2 deletions [64] as well as in a longitudinal study extending from childhood to young adulthood of patients who carry 22q11.2 deletions [41].

Given previous reports of volumetric changes in the frontal lobe of individuals with 22q11.2 deletions, we expected to also find a significant difference in the frontal lobe volume of *Df(16)A*$^{+/-}$ mice compared with WT littermates. However, the alteration in overall frontal lobe volume did not reach significance (q=0.18) (Supplementary Table 1). Interestingly, when we looked at left/right asymmetry, the left side of the frontal lobe was significantly increased in relative volume (q=0.10) while the right frontal lobe remained unchanged (q=0.54) (Figure 2H). Synaptic and long-range connection deficits have been previously described within the frontal lobe of *Df(16)A*$^{+/-}$ mice, including microscopic structural abnormalities in dendritic complexity, spine density, and cell density in specific cortical layers [10, 12, 13] (Fénelon K, MK, JAG unpublished observations). Given the abundance of evidence for cytoarchitectural abnormalities in combination with the previously observed volumetric alterations of the frontal lobe from human MR imaging studies, we examined volumetric changes in the *Df(16)A*$^{+/-}$ mice on a voxel-wise basis solely in the frontal lobe, thus decreasing the number of statistical comparisons and highlighting significant differences within the frontal lobe. Figure 5 highlights specific locations within the frontal lobe where volumetric differences are observed. Several areas within the frontal cortex were either decreased or increased in volume in the *Df(16)A*$^{+/-}$ mice compared with WT littermates. One of the subregions where a volumetric deficits was observed was the frontal association cortex, where we have previously also identified significant microscopic abnormalities in spine turnover (Fénelon K, MK, JAG unpublished observations). Notably, such opposing volumetric changes may also explain the lack of an overall significant finding across the frontal cortex as a whole. Indeed, co-existence of divergent volumetric changes of specific frontal lobe subregions is highly consistent with several neuroimaging studies on human subjects who carry the 22q11.2 deletion [50, 51].

Discussion

There have been an increasing number of quantitative MR imaging studies on human subjects who carry the 22q11.2 deletion (Table 1). In particular, the total brain volume in

individuals with 22q11.2 deletions has been reported to be smaller compared to healthy controls [43, 59, 60]. Furthermore, although not consistent across all human studies, some studies have demonstrated a larger reduction in white matter volume as compared to gray matter [37, 43, 60] while one study reported reduction in gray matter in 22q11.2 deletion carriers with schizophrenia [59]. In the *Df(16)A*$^{+/-}$ mice, we found no difference in the overall brain volume, including the total volume of gray or white matter (data not shown). However, in terms of specific brain regions, a number of consistent findings have emerged from neuroimaging studies of 22q11.2 deletion carriers. These include cortical atrophy, enlarged ventricles, midline deficits, increase in striatal volume, cerebellar atrophy, and white matter hyperintensities [36, 43, 51]. Many of the affected brain regions, such as the frontal and cerebellar cortex as well as the striatum, have also been implicated in the development of schizophrenia as well as in other behavioral and neurological phenotypes found in 22q11.2 deletion carriers. Importantly, a large number of these findings are faithfully recapitulated in the brain of *Df(16)A*$^{+/-}$ mice.

The striatal finding in individuals carrying a 22q11.2 deletion has been reported as both an increase in size and asymmetry of the caudate nucleus [49, 51]. The striatal region abnormality in the *Df(16)A*$^{+/-}$ mice was one of the strongest findings, with a 5.7% increase in relative volume (FDR = 5%). Using voxel-wise analysis, although there was a trend towards striatal asymmetry (left > right), this did not reach the level of significance.

In parallel with the striatal enlargement, globus pallidus volume was also found to be increased in *Df(16)A*$^{+/-}$ mice (+5.1%, FDR = 7%). The basal ganglia have been implicated in a wide range of neurological and neuropsychiatric disorders, including movement disorders and obsessive-compulsive disorder (OCD). In a subgroup of patients with OCD, neuroimaging studies have demonstrated a volumetric increase of the basal ganglia [79]. Notably, 22q11.2 deletion carriers have been reported to have higher rates of obsessive-compulsive disorder [80]. Obsessive-compulsive disorder in childhood was also found to be predictive of developing schizophrenia later in life in carriers of the 22q11.2 deletion [41].

Interestingly, increased striatal volumes and a reversed right > left asymmetry have both been reported reported in patients with attention-deficit hyperactivity disorder (ADHD) who are known to carry a 22q11.2 deletion [49], as well as in patients with ADHD in general, with unknown 22q11.2 deletion carrier status [81]. Moreover, it has previously been established that motor functioning is often impaired in children with 22q11.2 deletions. This includes both a developmental delay in motor milestones as well as deficits in motor function, which do not correlate with age (*e.g.*, visual-motor integration skills) and thus appear to reflect impaired motor function independent of any developmental delay [82]. These motor deficits could be the consequence of abnormalities in the cerebellum, basal ganglia and striatum, which together with the dorsolateral prefrontal cortex form a functionally interconnected neurocircuit. Notably, all these brain structures demonstrate volumetric changes in both human 22q11.2 deletion carriers and *Df(16)A*$^{+/-}$. Therefore, these specific volumetric abnormalities could underlie the motor deficits seen in human subjects with 22q11.2 deletions.

In the *Df(16)A*$^{+/-}$ mice, the volumes of the lateral ventricles, as well as the third and fourth ventricles were measured. Only the third ventricle (Figure 1) showed a statistically significant change in volume, with an increase in relative volume of 11% (q = 0.07); the lateral ventricle was also increased in size (8%, q = 0.47), but this was not a statistically significant difference. Interestingly, although ventricular enlargement is not specific to the 22q11.2 deletion, it is a common neuroanatomical finding in subjects with the microdeletion, especially when they are also diagnosed with schizophrenia [36] and ventricular enlargement is the most common finding reported in patients with schizophrenia [83]. Notably, of the entire ventricular system, the third ventricle is most frequently increased in volume in patients with schizophrenia [83].

Cerebellar alterations have been extensively linked to the 22q11.2 deletion in humans. Twelve different studies have reported cerebellar decrease in 22q11.2 deletion carriers with schizophrenia (Table 1) and five additional studies have found cerebellar decreases in individuals with schizophrenia in general. The majority of these studies do not address in detail the specific location of these differences within the cerebellum, but rather, report only the overall difference. Using a mouse model with demonstrated face validity is therefore advantageous since the resolution and ability to detect very subtle differences is dramatically increased compared with neuroimaging in human subjects [19]. The cerebellar findings in *Df(16)A*$^{+/-}$ mice are particularly instructive as they are localized to specific areas within both the deep cerebellar nuclei and the cerebellar cortex. The cerebellar cortex in the *Df(16)A*$^{+/-}$ mice was 5% smaller than WT littermates, whereas the arbor vita of the cerebellum (*i.e.,* the white matter of the cerebellum including the deep cerebellar nuclei) was not significantly different (q=0.27). However, within both of these regions, many voxel-wise differences were found (Figure 1H–I): lobule IV/V in the anterior lobes and lobules IX and X in the posterior lobes demonstrated a more precise localization of the previously reported overall volumetric decrease. Furthermore, the most striking finding was a highly robust bilateral reduction in size of both the cerebellar flocculous and para-flocculus of the cerebellum. Although most imaging studies typically do not assess individual cerebellar subregions, the flocculus – which is part of the cerebellar tonsil – was previously observed to be significantly smaller in children who carry a 22q11.2 deletion [40] as well as patients with first-episode schizophrenia [84]. Furthermore, in the *Df(16)A*$^{+/-}$ mice, we observed a decrease in volume of the vermis lobule IV/V, representing the caudal portion of the anterior lobe, the vermis X (nodulus), the flocculus and paraflocculus that together are known to be involved in the execution of smooth pursuit eye movements [85]. Additionally, the vestibulocerebellar and superior vestibular nuclei were decreased in volume. As both nuclei and lobules are part of the vestibulo-cerebellar pathway, these structures receive sensory input through the vestibular tracts regarding balance and help facilitate eye movements through efferent connections. It is striking that several of these cerebellar structures, which together form a functional neurocircuitry unit responsible for smooth pursuit eye movements, are affected both in human subjects with 22q11.2 deletions as well as the *Df(16)A*$^{+/-}$ mice. In concordance with this observation, abnormalities in smooth pursuit eye movements have been described in subjects with a 22q11.2 deletion [86] as well as in patients with polymorphisms of *COMT* [87] and *ZDHHC8* [88], both of which are genes within the 22q11.2 locus [89]. Of note, impairment in smooth pursuit eye movements is one of the most

widely replicated findings in schizophrenia and is also more prevalent in unaffected first-degree relatives of patients with schizophrenia [90]. Furthermore, the cerebellum communicates with the frontal cortex via polysynaptic circuits, forming a complex topography. In the *Df(16)A*$^{+/-}$ mice, we observed bilateral volume reductions in the medial portions of the anterior lobule and dorsal surface of crus I lobule. Both regions connect through the thalamus to the cerebral cortex and back to the cerebellum via the pontine nuclei [91]. Involvement in the executive control network has been shown for crus I in humans [92] whereas the anterior portion of lobule IV/V has been linked to sensorimotor tasks, involving especially the upper extremities [92-94].

The reduction of the anterior section of the amygdala in the *Df(16)A*$^{+/-}$ mice is another finding which is consistent with the human neuroanatomical phenotype associated with the 22q11.2 deletion. The most consistent data has demonstrated a decrease in amygdala volume in individuals with 22q11.2 deletions [64], which persists into adulthood [41]. The amygdala is known to be part of a microcircuit that gates conditioned fear across species [95]. Interestingly, *Df(16)A*$^{+/-}$ mice exhibit robust deficits in both cued and contextual fear memory compared with WT littermates, with the cued version of the test requiring intact functioning of the amygdala while the context version of the test typically requires both hippocampus and amygdala. It could therefore be that the volumetric reduction of the anterior portion of the amygdala is associated with increased anxiety disorders [96] as well as cognitive deficits [1] in human subjects with 22q11.2 deletions. Furthermore, an event-related functional MR imaging study has also demonstrated a lack of repetition-suppression effect for fearful faces in the right amygdala in individuals with 22q11.2 deletions, suggesting a lack of amygdala modulation of fear expression in human subjects who carry the deletion [97]. A reduction in amygdala volume [65], decreased activation in the amygdala during emotional face processing [98], and cognitive deficits such as abnormalities in fear conditioning [99] have all been described in individuals with schizophrenia. Moreover, amygdala expression of *Sept5*, a gene in the human 22q11.2 locus and the syntenic murine *Df16A* region, has been identified as a possible determinant of impaired social interaction in psychiatric disorders such as schizophrenia [100].

Differences in frontal lobe size have been reported consistently in both children and adults with the 22q11.2 deletion [42, 50, 51]. Unlike striatal and cerebellar findings, however, reports have been inconsistent. Eliez et al. (2002) reported an increase in the relative volume of frontal lobe in children with the 22q11.2 deletion; however, Kates et al. (2004) found that absolute frontal lobe volumes were smaller in children with 22q11.2 deletions. The relative volume of the frontal lobe was increased in the *Df(16)A*$^{+/-}$ compared to WT littermates (+3.2%, q = 0.18), although not statistically significant. We did examine voxel-wise differences within the frontal lobe, however, and there were specific regions where statistically significant differences were found (Figure 3). Specifically within the frontal lobe, we identified areas that were either significantly enlarged or decreased for which we hypothesize that such contrasting differences could be responsible for the discrepancies between studies arising from competing effects. Some of the imaging studies of 22q11.2 deletion carriers have also demonstrated volumetric changes in the parietal, temporal and occipital lobes, most of which were reported to be a loss of volume [70]. The volumetric

alterations described in these studies have not always been consistent and in the *Df(16)A*$^{+/-}$ mice we observe no significant changes in any of these 3 cortical regions (Supplementary Table 1).

Together, we identify a striking similarity in the specific volumetric changes of *Df(16)A*$^{+/-}$ mice compared with human 22q11.2 deletion patients, including cortico-cerebellar, cortico-striatal, and cortico-limbic circuits. Functional abnormalities in these critical neural circuitry would likely lead to defective information processing, cognitive and motor deficits, and perhaps result in psychosis. Moreover, taken together, the MRI data of the *Df(16)A*$^{+/-}$ mutant mice that we present in this study clearly demonstrates the face validity of this model since it captures several of the fundamental neuroanatomical characteristics of the 22q11.2 deletion. As such, neuroimaging findings in *Df(16)A*$^{+/-}$ mice will help guide the design and interpretation of additional complementary studies, such as functional imaging studies and higher resolution cytoarchitectural analysis of the affected regions, thereby advancing our understanding of the critical pathogenic mechanisms of abnormal brain development, which ultimately lead to the emergence of 22q11.2 deletion-associated psychiatric and cognitive symptoms. This may facilitate development and testing of new treatments by evaluating the effect of these medications on the neuroanatomical abnormalities in both man and mouse.

Supplementary Material

Refer to Web version on PubMed Central for supplementary material.

ACKNOWLEDGEMENTS

We would like to thank Louise van der Weerd for helpful discussions during the initial phase of this project and Christine LaLiberté, Kim Stark, and Matthijs van Eede for their assistance with aspects of the MRI scanning and analysis. We would also like to acknowledge the Ontario Mental Health Foundation (OHMF) for salary support (J.E.). This work was supported by grants from the US National Institute of Mental Health, Grants MH67068 (to M.K. and J.A.G.) and MH077235 (to J.A.G.), and the Canadian Institute for Health Research (CIHR) and the Ontario Brain Institute (OBI).

References

1. Karayiorgou M, Simon TJ, Gogos JA. 22q11.2 microdeletions: linking DNA structural variation to brain dysfunction and schizophrenia. Nat Rev Neurosci. 2010; 11:402–416. [PubMed: 20485365]
2. Levinson DF, Shi J, Wang K, Oh S, Riley B, Pulver AE, et al. Genome-wide association study of multiplex schizophrenia pedigrees. Am J Psychiatry. 2012; 169:963–973. [PubMed: 22885689]
3. Karayiorgou M, Morris MA, Morrow B, Shprintzen RJ, Goldberg R, Borrow J, et al. Schizophrenia susceptibility associated with interstitial deletions of chromosome 22q11. Proc Natl Acad Sci USA. 1995; 92:7612–7616. [PubMed: 7644464]
4. Xu B, Roos JL, Levy S, van Rensburg EJ, Gogos JA, Karayiorgou M. Strong association of de novo copy number mutations with sporadic schizophrenia. Nat Genet. 2008; 40:880–885. [PubMed: 18511947]
5. Sebat J, Lakshmi B, Malhotra D, Troge J, Lese-Martin C, Walsh T, et al. Strong association of de novo copy number mutations with autism. Science. 2007; 316:445–449. [PubMed: 17363630]
6. Malhotra D, McCarthy S, Michaelson JJ, Vacic V, Burdick KE, Yoon S, et al. High frequencies of de novo CNVs in bipolar disorder and schizophrenia. Neuron. 2011; 72:951–963. [PubMed: 22196331]

7. Stark KL, Xu B, Bagchi A, Lai W-S, Liu H, Hsu R, et al. Altered brain microRNA biogenesis contributes to phenotypic deficits in a 22q11-deletion mouse model. Nat Genet. 2008; 40:751–760. [PubMed: 18469815]
8. Mukai J, Dhilla A, Drew LJ, Stark KL, Cao L, Macdermott AB, et al. Palmitoylation-dependent neurodevelopmental deficits in a mouse model of 22q11 microdeletion. Nat Neurosci. 2008; 11:1302–1310. [PubMed: 18836441]
9. Sigurdsson T, Stark KL, Karayiorgou M, Gogos JA, Gordon JA. Impaired hippocampal-prefrontal synchrony in a genetic mouse model of schizophrenia. Nature. 2010; 464:763–767. [PubMed: 20360742]
10. Fénelon K, Mukai J, Xu B, Hsu P-K, Drew LJ, Karayiorgou M, et al. Deficiency of Dgcr8, a gene disrupted by the 22q11.2 microdeletion, results in altered short-term plasticity in the prefrontal cortex. Proc Natl Acad Sci USA. 2011; 108:4447–4452. [PubMed: 21368174]
11. Drew LJ, Stark KL, Fénelon K, Karayiorgou M, Macdermott AB, Gogos JA. Evidence for altered hippocampal function in a mouse model of the human 22q11.2 microdeletion. Mol Cell Neurosci. 2011; 47:293–305. [PubMed: 21635953]
12. Xu B, Ionita-Laza I, Roos JL, Boone B, Woodrick S, Sun Y, et al. De novo gene mutations highlight patterns of genetic and neural complexity in schizophrenia. Nat Genet. 2012; 44:1365–1369. [PubMed: 23042115]
13. Drew LJ, Crabtree GW, Markx S, Stark KL, Chaverneff F, Xu B, et al. The 22q11.2 microdeletion: fifteen years of insights into the genetic and neural complexity of psychiatric disorders. Int J Dev Neurosci. 2011; 29:259–281. [PubMed: 20920576]
14. Arguello PA, Gogos JA. Modeling madness in mice: one piece at a time. Neuron. 2006; 52:179–196. [PubMed: 17015235]
15. Zhang J, Peng Q, Li Q, Jahanshad N, Hou Z, Jiang M, et al. Longitudinal characterization of brain atrophy of a Huntington's disease mouse model by automated morphological analyses of magnetic resonance images. Neuroimage. 2010; 49:2340–2351. [PubMed: 19850133]
16. Cramer PE, Cirrito JR, Wesson DW, Lee CYD, Karlo JC, Zinn AE, et al. ApoE-directed therapeutics rapidly clear β-amyloid and reverse deficits in AD mouse models. Science. 2012; 335:1503–1506. [PubMed: 22323736]
17. Goldberg MS, Pisani A, Haburcak M, Vortherms TA, Kitada T, Costa C, et al. Nigrostriatal dopaminergic deficits and hypokinesia caused by inactivation of the familial Parkinsonism-linked gene DJ-1. Neuron. 2005; 45:489–496. [PubMed: 15721235]
18. Lerch JP, Yiu AP, Martinez-Canabal A, Pekar T, Bohbot VD, Frankland PW, et al. Maze training in mice induces MRI-detectable brain shape changes specific to the type of learning. Neuroimage. 2011; 54:2086–2095. [PubMed: 20932918]
19. Nieman BJ, Wong MD, Henkelman RM. Genes into geometry: imaging for mouse development in 3D. Current Opinion in Genetics & Development. 2011; 21:638–646. [PubMed: 21907568]
20. Nieman BJ, Lerch JP, Bock NA, Chen XJ, Sled JG, Henkelman RM. Mouse behavioral mutants have neuroimaging abnormalities. Hum Brain Mapp. 2007; 28:567–575. [PubMed: 17437292]
21. Ellegood J, Pacey LK, Hampson DR, Lerch JP, Henkelman RM. Anatomical phenotyping in a mouse model of fragile X syndrome with magnetic resonance imaging. Neuroimage. 2010; 53:1023–1029. [PubMed: 20304074]
22. Horev G, Ellegood J, Lerch JP, Son Y-EE, Muthuswamy L, Vogel H, et al. Dosage-dependent phenotypes in models of 16p11.2 lesions found in autism. Proc Natl Acad Sci USA. 2011; 108:17076–17081. [PubMed: 21969575]
23. Ellegood J, Lerch JP, Henkelman RM. Brain abnormalities in a Neuroligin3 R451C knockin mouse model associated with autism. Autism Res. 2011; 4:368–376. [PubMed: 21882360]
24. Tan GM, Arnone D, McIntosh AM, Ebmeier KP. Meta-analysis of magnetic resonance imaging studies in chromosome 22q11.2 deletion syndrome (velocardiofacial syndrome). Schizophrenia Research. 2009; 115:173–181. [PubMed: 19819113]
25. Johnson GA, Cofer GP, Fubara B, Gewalt SL, Hedlund LW, Maronpot RR. Magnetic resonance histology for morphologic phenotyping. J Magn Reson Imaging. 2002; 16:423–429. [PubMed: 12353257]

26. Lerch JP, Sled JG, Henkelman RM. MRI phenotyping of genetically altered mice. Methods Mol Biol. 2011; 711:349–361. [PubMed: 21279611]
27. Dazai J, Spring S, Cahill LS, Henkelman RM. Multiple-mouse neuroanatomical magnetic resonance imaging. J Vis Exp. 2011
28. Thomas DL, De Vita E, Roberts S, Turner R, Yousry TA, Ordidge RJ. High-resolution fast spin echo imaging of the human brain at 4.7 T: implementation and sequence characteristics. Magn Reson Med. 2004; 51:1254–1264. [PubMed: 15170847]
29. Collins DL, Neelin P, Peters TM, Evans AC. Automatic 3D intersubject registration of MR volumetric data in standardized Talairach space. J Comput Assist Tomogr. 1994; 18:192–205. [PubMed: 8126267]
30. Avants BB, Epstein CL, Grossman M, Gee JC. Symmetric diffeomorphic image registration with cross-correlation: evaluating automated labeling of elderly and neurodegenerative brain. Med Image Anal. 2008; 12:26–41. [PubMed: 17659998]
31. Avants BB, Tustison NJ, Song G, Cook PA, Klein A, Gee JC. A reproducible evaluation of ANTs similarity metric performance in brain image registration. Neuroimage. 2011; 54:2033–2044. [PubMed: 20851191]
32. Nieman BJ, Flenniken AM, Adamson SL, Henkelman RM, Sled JG. Anatomical phenotyping in the brain and skull of a mutant mouse by magnetic resonance imaging and computed tomography. Physiol Genomics. 2006; 24:154–162. [PubMed: 16410543]
33. Dorr AE, Lerch JP, Spring S, Kabani N, Henkelman RM. High resolution three-dimensional brain atlas using an average magnetic resonance image of 40 adult C57Bl/6J mice. Neuroimage. 2008; 42:60–69. [PubMed: 18502665]
34. Genovese CR, Lazar NA, Nichols T. Thresholding of statistical maps in functional neuroimaging using the false discovery rate. Neuroimage. 2002; 15:870–878. [PubMed: 11906227]
35. Smith SM, Nichols TE. Threshold-free cluster enhancement: addressing problems of smoothing, threshold dependence and localisation in cluster inference. Neuroimage. 2009; 44:83–98. [PubMed: 18501637]
36. Chow EW, Mikulis DJ, Zipursky RB, Scutt LE, Weksberg R, Bassett AS. Qualitative MRI findings in adults with 22q11 deletion syndrome and schizophrenia. BPS. 1999; 46:1436–1442.
37. van Amelsvoort T, Daly E, Robertson D, Suckling J, Ng V, Critchley H, et al. Structural brain abnormalities associated with deletion at chromosome 22q11: quantitative neuroimaging study of adults with velo-cardio-facial syndrome. Br J Psychiatry. 2001; 178:412–419. [PubMed: 11331556]
38. Eliez S, Schmitt JE, White CD, Wellis VG, Reiss AL. A quantitative MRI study of posterior fossa development in velocardiofacial syndrome. BPS. 2001; 49:540–546.
39. van Amelsvoort T, Daly E, Henry J, Robertson D, Ng V, Owen M, et al. Brain anatomy in adults with velocardiofacial syndrome with and without schizophrenia: preliminary results of a structural magnetic resonance imaging study. Arch Gen Psychiatry. 2004; 61:1085–1096. [PubMed: 15520356]
40. Bish JP, Pendyal A, Ding L, Ferrante H, Nguyen V, McDonald-McGinn D, et al. Specific cerebellar reductions in children with chromosome 22q11.2 deletion syndrome. Neurosci Lett. 2006; 399:245–248. [PubMed: 16517069]
41. Gothelf D, Michaelovsky E, Frisch A, Zohar AH, Presburger G, Burg M, et al. Association of the low-activity COMT 158Met allele with ADHD and OCD in subjects with velocardiofacial syndrome. Int J Neuropsychopharmacol. 2007; 10:301–308. [PubMed: 16734939]
42. Shashi V, Kwapil TR, Kaczorowski J, Berry MN, Santos CS, Howard TD, et al. Evidence of gray matter reduction and dysfunction in chromosome 22q11.2 deletion syndrome. Psychiatry Res. 2010; 181:1–8. [PubMed: 19962860]
43. Kates WR, Bansal R, Fremont W, Antshel KM, Hao X, Higgins AM, et al. Mapping cortical morphology in youth with velocardiofacial (22q11.2 deletion) syndrome. J Am Acad Child Adolesc Psychiatry. 2011; 50:272–282.e272. [PubMed: 21334567]
44. Rimol LM, Hartberg CB, Nesvåg R, Fennema-Notestine C, Hagler DJ, Pung CJ, et al. Cortical thickness and subcortical volumes in schizophrenia and bipolar disorder. Biological Psychiatry. 2010; 68:41–50. [PubMed: 20609836]

45. Watson DR, Anderson JME, Bai F, Barrett SL, McGinnity TM, Mulholland CC, et al. A voxel based morphometry study investigating brain structural changes in first episode psychosis. Behavioural Brain Research. 2012; 227:91–99. [PubMed: 22056751]
46. Greenstein D, Lenroot R, Clausen L, Chavez A, Vaituzis AC, Tran L, et al. Cerebellar development in childhood onset schizophrenia and non-psychotic siblings. Psychiatry Res. 2011; 193:131–137. [PubMed: 21803550]
47. Bergé D, Carmona S, Rovira M, Bulbena A, Salgado P, Vilarroya O. Gray matter volume deficits and correlation with insight and negative symptoms in first-psychotic-episode subjects. Acta Psychiatr Scand. 2011; 123:431–439. [PubMed: 21054282]
48. Borgwardt SJ, Picchioni MM, Ettinger U, Toulopoulou T, Murray R, McGuire PK. Regional gray matter volume in monozygotic twins concordant and discordant for schizophrenia. Biological Psychiatry. 2010; 67:956–964. [PubMed: 20006324]
49. Sugama S, Bingham PM, Wang PP, Moss EM, Kobayashi H, Eto Y. Morphometry of the head of the caudate nucleus in patients with velocardiofacial syndrome (del 22q11.2). Acta Paediatr. 2000; 89:546–549. [PubMed: 10852189]
50. Kates WR, Burnette CP, Bessette BA, Folley BS, Strunge L, Jabs EW, et al. Frontal and caudate alterations in velocardiofacial syndrome (deletion at chromosome 22q11.2). J Child Neurol. 2004; 19:337–342. [PubMed: 15224707]
51. Eliez S, Barnea-Goraly N, Schmitt JE, Liu Y, Reiss AL. Increased basal ganglia volumes in velo-cardio-facial syndrome (deletion 22q11.2). BPS. 2002; 52:68–70.
52. Goldman AL, Pezawas L, Mattay VS, Fischl B, Verchinski BA, Zoltick B, et al. Heritability of brain morphology related to schizophrenia: a large-scale automated magnetic resonance imaging segmentation study. Biological Psychiatry. 2008; 63:475–483. [PubMed: 17727823]
53. Mamah D, Wang L, Barch D, de Erausquin GA, Gado M, Csernansky JG. Structural analysis of the basal ganglia in schizophrenia. Schizophrenia Research. 2007; 89:59–71. [PubMed: 17071057]
54. Chakos MH, Lieberman JA, Bilder RM, Borenstein M, Lerner G, Bogerts B, et al. Increase in caudate nuclei volumes of first-episode schizophrenic patients taking antipsychotic drugs. Am J Psychiatry. 1994; 151:1430–1436. [PubMed: 7916539]
55. Sieberer M, Haltenhof H, Haubitz B, Pabst B, Miller K, Garlipp P. Basal ganglia calcification and psychosis in 22q11.2 deletion syndrome. Eur Psychiatry. 2005; 20:567–569. [PubMed: 15967641]
56. Cao Z, Yu R, Dun K, Burke J, Caplin N, Greenaway T. 22q11.2 deletion presenting with severe hypocalcaemia, seizure and basal ganglia calcification in an adult man. Intern Med J. 2011; 41:63–66. [PubMed: 21265963]
57. Hokama H, Shenton ME, Nestor PG, Kikinis R, Levitt JJ, Metcalf D, et al. Caudate, putamen, and globus pallidus volume in schizophrenia: a quantitative MRI study. Psychiatry Res. 1995; 61:209–229. [PubMed: 8748466]
58. Arnone D, Cavanagh J, Gerber D, Lawrie SM, Ebmeier KP, McIntosh AM. Magnetic resonance imaging studies in bipolar disorder and schizophrenia: meta-analysis. Br J Psychiatry. 2009; 195:194–201. [PubMed: 19721106]
59. Chow EWC, Zipursky RB, Mikulis DJ, Bassett AS. Structural brain abnormalities in patients with schizophrenia and 22q11 deletion syndrome. BPS. 2002; 51:208–215.
60. Eliez S, Schmitt JE, White CD, Reiss AL. Children and adolescents with velocardiofacial syndrome: a volumetric MRI study. Am J Psychiatry. 2000; 157:409–415. [PubMed: 10698817]
61. Simon TJ, Ding L, Bish JP, McDonald-McGinn DM, Zackai EH, Gee J. Volumetric, connective, and morphologic changes in the brains of children with chromosome 22q11.2 deletion syndrome: an integrative study. Neuroimage. 2005; 25:169–180. [PubMed: 15734353]
62. Galderisi S, Quarantelli M, Volpe U, Mucci A, Cassano GB, Invernizzi G, et al. Patterns of structural MRI abnormalities in deficit and nondeficit schizophrenia. Schizophr Bull. 2008; 34:393–401. [PubMed: 17728266]
63. Styner M, Lieberman JA, McClure RK, Weinberger DR, Jones DW, Gerig G. Morphometric analysis of lateral ventricles in schizophrenia and healthy controls regarding genetic and disease-specific factors. Proc Natl Acad Sci USA. 2005; 102:4872–4877. [PubMed: 15772166]

64. Deboer T, Wu Z, Lee A, Simon TJ. Hippocampal volume reduction in children with chromosome 22q11.2 deletion syndrome is associated with cognitive impairment. Behav Brain Funct. 2007; 3:54. [PubMed: 17956622]

65. Namiki C, Hirao K, Yamada M, Hanakawa T, Fukuyama H, Hayashi T, et al. Impaired facial emotion recognition and reduced amygdalar volume in schizophrenia. Psychiatry Res. 2007; 156:23–32. [PubMed: 17728113]

66. Exner C, Boucsein K, Degner D, Irle E, Weniger G. Impaired emotional learning and reduced amygdala size in schizophrenia: a 3-month follow-up. Schizophrenia Research. 2004; 71:493–503. [PubMed: 15474920]

67. Yoshida T, McCarley RW, Nakamura M, Lee K, Koo M-S, Bouix S, et al. A prospective longitudinal volumetric MRI study of superior temporal gyrus gray matter and amygdala-hippocampal complex in chronic schizophrenia. Schizophrenia Research. 2009; 113:84–94. [PubMed: 19524408]

68. James AC, James S, Smith DM, Javaloyes A. Cerebellar, prefrontal cortex, and thalamic volumes over two time points in adolescent-onset schizophrenia. Am J Psychiatry. 2004; 161:1023–1029. [PubMed: 15169690]

69. Yoshihara Y, Sugihara G, Matsumoto H, Suckling J, Nishimura K, Toyoda T, et al. Voxel-based structural magnetic resonance imaging (MRI) study of patients with early onset schizophrenia. Ann Gen Psychiatry. 2008; 7:25. [PubMed: 19102744]

70. Bearden CE, van Erp TGM, Dutton RA, Tran H, Zimmermann L, Sun D, et al. Mapping cortical thickness in children with 22q11.2 deletions. Cereb Cortex. 2007; 17:1889–1898. [PubMed: 17056649]

71. Cascella NG, Fieldstone SC, Rao VA, Pearlson GD, Sawa A, Schretlen DJ. Gray-matter abnormalities in deficit schizophrenia. Schizophrenia Research. 2010; 120:63–70. [PubMed: 20452187]

72. Mané A, Falcon C, Mateos JJ, Fernandez-Egea E, Horga G, Lomeña F, et al. Progressive gray matter changes in first episode schizophrenia: a 4-year longitudinal magnetic resonance study using VBM. Schizophrenia Research. 2009; 114:136–143. [PubMed: 19683418]

73. Neckelmann G, Specht K, Lund A, Ersland L, Smievoll AI, Neckelmann D, et al. Mr morphometry analysis of grey matter volume reduction in schizophrenia: association with hallucinations. Int J Neurosci. 2006; 116:9–23. [PubMed: 16318996]

74. Douaud G, Mackay C, Andersson J, James S, Quested D, Ray MK, et al. Schizophrenia delays and alters maturation of the brain in adolescence. Brain. 2009; 132:2437–2448. [PubMed: 19477963]

75. Rotarska-Jagiela A, Oertel-Knoechel V, DeMartino F, van de Ven V, Formisano E, Roebroeck A, et al. Anatomical brain connectivity and positive symptoms of schizophrenia: a diffusion tensor imaging study. Psychiatry Res. 2009; 174:9–16. [PubMed: 19767179]

76. Turetsky BI, Moberg PJ, Yousem DM, Doty RL, Arnold SE, Gur RE. Reduced olfactory bulb volume in patients with schizophrenia. Am J Psychiatry. 2000; 157:828–830. [PubMed: 10784482]

77. Nopoulos PC, Ceilley JW, Gailis EA, Andreasen NC. An MRI study of midbrain morphology in patients with schizophrenia: relationship to psychosis, neuroleptics, and cerebellar neural circuitry. BPS. 2001; 49:13–19.

78. Koolschijn PCMP, van Haren NEM, Hulshoff Pol HE, Kahn RS. Hypothalamus volume in twin pairs discordant for schizophrenia. European Neuropsychopharmacology. 2008; 18:312–315. [PubMed: 18222652]

79. Giedd JN, Rapoport JL, Garvey MA, Perlmutter S, Swedo SE. MRI assessment of children with obsessive-compulsive disorder or tics associated with streptococcal infection. Am J Psychiatry. 2000; 157:281–283. [PubMed: 10671403]

80. Karayiorgou M, Sobin C, Blundell ML, Galke BL, Malinova L, Goldberg P, et al. Family-based association studies support a sexually dimorphic effect of COMT and MAOA on genetic susceptibility to obsessive-compulsive disorder. BPS. 1999; 45:1178–1189.

81. Garrett A, Penniman L, Epstein JN, Casey BJ, Hinshaw SP, Glover G, et al. Neuroanatomical abnormalities in adolescents with attention-deficit/hyperactivity disorder. J Am Acad Child Adolesc Psychiatry. 2008; 47:1321–1328. [PubMed: 18827721]

82. Sobin C, Kiley-Brabeck K, Daniels S, Khuri J, Taylor L, Blundell M, et al. Neuropsychological characteristics of children with the 22q11 Deletion Syndrome: a descriptive analysis. Child Neuropsychol. 2005; 11:39–53. [PubMed: 15823982]

83. Shenton ME, Dickey CC, Frumin M, McCarley RW. A review of MRI findings in schizophrenia. Schizophrenia Research. 2001; 49:1–52. [PubMed: 11343862]

84. Rasser PE, Schall U, Peck G, Cohen M, Johnston P, Khoo K, et al. Cerebellar grey matter deficits in first-episode schizophrenia mapped using cortical pattern matching. Neuroimage. 2010; 53:1175–1180. [PubMed: 20633666]

85. Ilg UJ, Thier P. The neural basis of smooth pursuit eye movements in the rhesus monkey brain. Brain Cogn. 2008; 68:229–240. [PubMed: 18835077]

86. Vorstman JAS, Turetsky BI, Sijmens-Morcus MEJ, de Sain MG, Dorland B, Sprong M, et al. Proline affects brain function in 22q11DS children with the low activity COMT 158 allele. Neuropsychopharmacology. 2009; 34:739–746. [PubMed: 18769474]

87. Park BL, Shin HD, Cheong HS, Park CS, Sohn J-W, Kim B-J, et al. Association analysis of COMT polymorphisms with schizophrenia and smooth pursuit eye movement abnormality. J Hum Genet. 2009; 54:709–712. [PubMed: 19881467]

88. Shin HD, Park BL, Bae JS, Park TJ, Chun JY, Park CS, et al. Association of ZDHHC8 polymorphisms with smooth pursuit eye movement abnormality. Am J Med Genet B Neuropsychiatr Genet. 2010; 153B:1167–1172. [PubMed: 20468065]

89. Mukai J, Liu H, Burt RA, Swor DE, Lai W-S, Karayiorgou M, et al. Evidence that the gene encoding ZDHHC8 contributes to the risk of schizophrenia. Nat Genet. 2004; 36:725–731. [PubMed: 15184899]

90. Levy DL, Sereno AB, Gooding DC, O'Driscoll GA. Eye tracking dysfunction in schizophrenia: characterization and pathophysiology. Curr Top Behav Neurosci. 2010; 4:311–347. [PubMed: 21312405]

91. Ramnani N. The primate cortico-cerebellar system: anatomy and function. Nat Rev Neurosci. 2006; 7:511–522. [PubMed: 16791141]

92. Stoodley CJ, Schmahmann JD. Functional topography in the human cerebellum: a meta-analysis of neuroimaging studies. Neuroimage. 2009; 44:489–501. [PubMed: 18835452]

93. Stoodley CJ, Valera EM, Schmahmann JD. Functional topography of the cerebellum for motor and cognitive tasks: an fMRI study. Neuroimage. 2012; 59:1560–1570. [PubMed: 21907811]

94. Arenz A, Bracey EF, Margrie TW. Sensory representations in cerebellar granule cells. Curr Opin Neurobiol. 2009; 19:445–451. [PubMed: 19651506]

95. Haubensak W, Kunwar PS, Cai H, Ciocchi S, Wall NR, Ponnusamy R, et al. Genetic dissection of an amygdala microcircuit that gates conditioned fear. Nature. 2010; 468:270–276. [PubMed: 21068836]

96. Fung WLA, McEvilly R, Fong J, Silversides C, Chow E, Bassett A. Elevated prevalence of generalized anxiety disorder in adults with 22q11.2 deletion syndrome. Am J Psychiatry. 2010; 167:998. [PubMed: 20693476]

97. Andersson F, Glaser B, Spiridon M, Debbané M, Vuilleumier P, Eliez S. Impaired activation of face processing networks revealed by functional magnetic resonance imaging in 22q11.2 deletion syndrome. Biological Psychiatry. 2008; 63:49–57. [PubMed: 17651704]

98. Gur RE, McGrath C, Chan RM, Schroeder L, Turner T, Turetsky BI, et al. An fMRI study of facial emotion processing in patients with schizophrenia. Am J Psychiatry. 2002; 159:1992–1999. [PubMed: 12450947]

99. Holt DJ, Coombs G, Zeidan MA, Goff DC, Milad MR. Failure of neural responses to safety cues in schizophrenia. Arch Gen Psychiatry. 2012; 69:893–903. [PubMed: 22945619]

100. Harper KM, Hiramoto T, Tanigaki K, Kang G, Suzuki G, Trimble W, et al. Alterations of social interaction through genetic and environmental manipulation of the 22q11.2 gene Sept5 in the mouse brain. Hum Mol Genet. 2012; 21:3489–3499. [PubMed: 22589251]

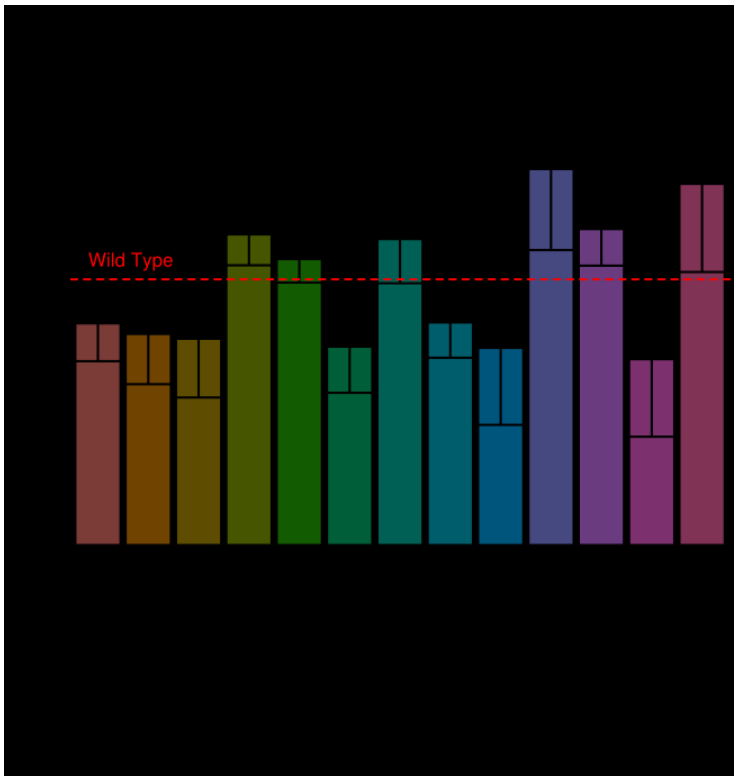

Figure 1.

Thirteen different regions in which the relative volume was significantly different in the *Df(16)A*$^{+/-}$ mice compared with WT littermates. The relative volumes in this graph were normalized to indicate how they differ from the average WT. Error bars display the standard deviation. A region was deemed significant at <15% FDR, 9 of these regions remained significant at a more stringent FDR of <10% (Supplementary Table 1).

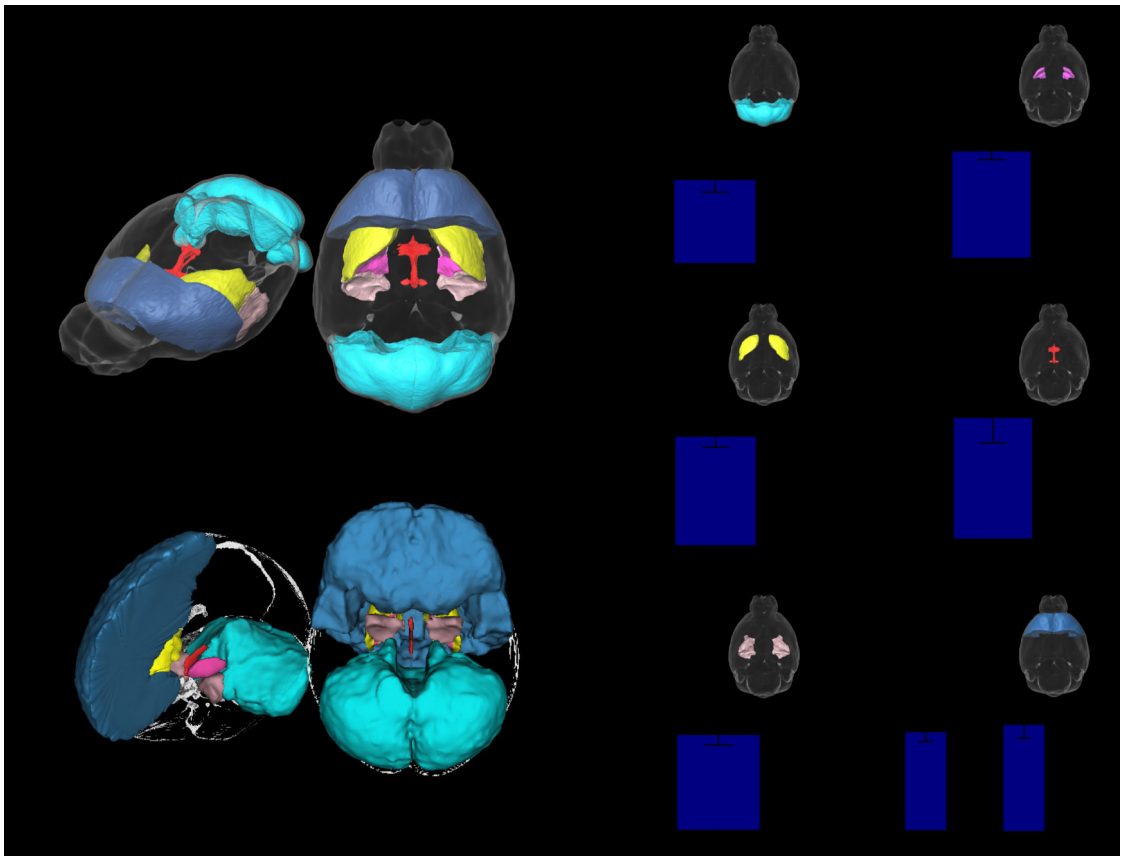

Figure 2.

Several regions are highlighted in 3D where similarities were found between the mouse (A) and human (B). The relative volume (% total brain volume) differences in these regions are highlighted in the bar graphs (C-H). Please note, the amygdala as a whole does not reach significance; however, highly significant decreases were found within subregions of the amygdala (seen in Figure 3). * indicates significance at <15% FDR, ** indicates significance at <10% FDR.

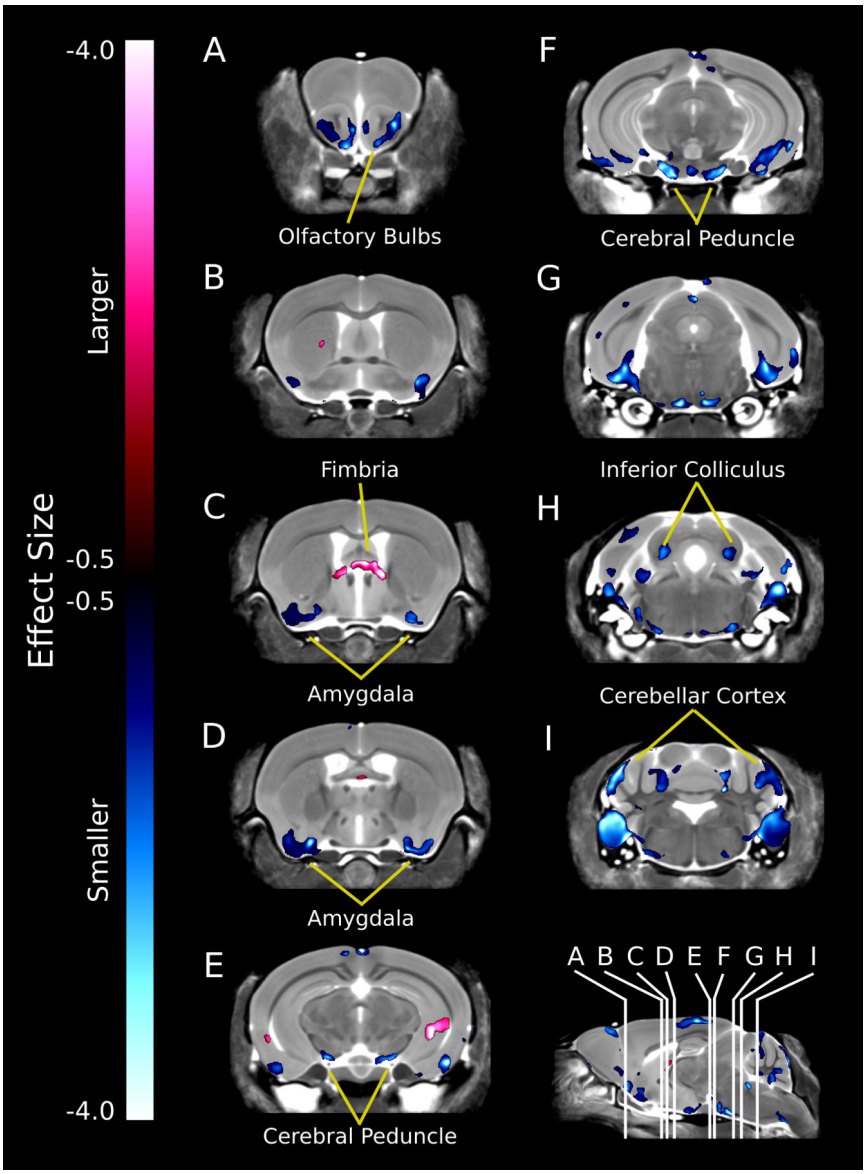

Figure 3.

Anterior (A) to posterior (I) coronal flythrough of the relative volume difference between the *Df(16)A*$^{+/-}$ mice and the corresponding WT littermates. Highlighted in red are the areas that were significantly larger and in blue the areas that are significantly smaller in the *Df(16)A*$^{+/-}$ mice. The locations of the coronal slices are displayed on the sagittal slice on the bottom-right.

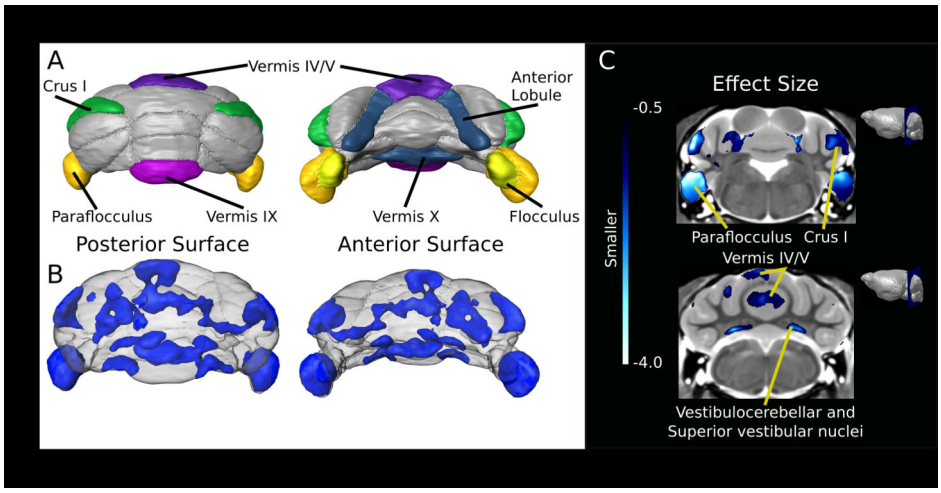

Figure 4.

Cerebellar differences found within the *Df16A*$^{+/-}$ mice. (A) Schematic surface renderings highlighting regions of interest (ROIs) including the anterior lobule representing the paravermis portions of vermis lobule IV/V, vermis lobules IX/X, crus I, paraflocculus and flocculus. (B) A 3D map of areas with an effect size above 0.5 that survived multiple comparisons using Threshold-free Cluster Enhancement (TFCE) (Smith *et al.* 2009). (C) Coronal slice of effect size representing smaller volumes within the cerebellum. Visible on the top slice are the anterior portion of lobule IV/V, crus I, paraflocculus and flocculus. The lower slice includes lobule IV/V within the vermis, left simplex lobule, and the superior vestibular and vestibulocerebellar nuclei.

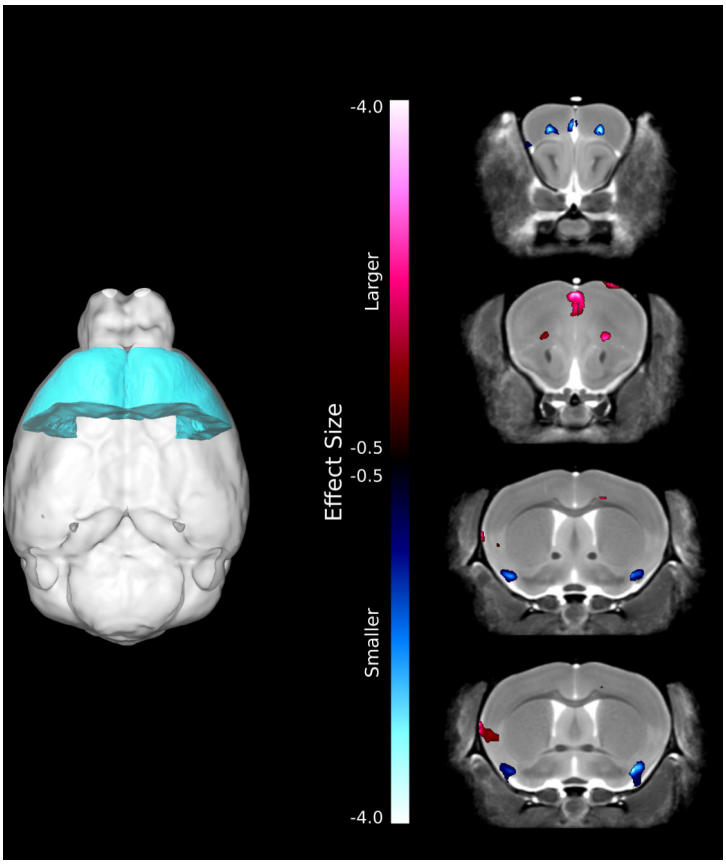

Figure 5.

(A) Highlighted is the frontal lobe, a region that commonly shows volumetric alterations in individuals with 22q11.2 microdeletions. B) Highlighted are the genotypic differences in relative volume within the frontal lobe region. Areas in red are significantly larger and areas in blue are significantly smaller in the *Df(16)A*$^{+/-}$ mice compared to WT littermates.

Table 1

Comparison between structural MRI findings of *Df16A*$^{+/-}$ mice and structural MRI findings in human subjects with 22q11.2 microdeletion

Brain structure	*Df16A*$^{+/-}$ mice	22q11.2 deletion carriers	References	SCZ patients	References
Cerebellum (cortex)	↓	↓	24, 36-43	↓	44-48
Striatum					
Caudate nucleus	↑	↑	41, 49-51		52-54
Globus pallidus	↑	Calcifications	51, 55, 56	↑	53, 57, 58
Ventricles	↑ (3rd ventricle)	↑	36, 59-61	↑	58, 62, 63
Amygdala	↓	↓	41, 64	↓	65-67
Frontal cortex	↓ (sub-regions)	↓	50, 59	↓	58, 68
Pontine nucleus	↓	Decreased volume of pons	38		69
Cuneate nucleus	↓	↓ (cuneus)	70		71-73
Corticospinal tracts (pyramids)	↓	None	N/A	↓	74, 75
Lateral olfactory tract	↓	None	N/A	↓ Olfactory bulb	76
Posterior commissure	↓	None	N/A	None	N/A
Superior olivary complex	↓	None	N/A	None	N/A
Midbrain	↓	Not significant	38	↓	77
Olfactory bulbs	↓	None	N/A	↓ Olfactory bulb	76
Hypothalamus	↓	None	N/A	↓	78